P10.8 SPATIAL PROPERTIES OF WIND DIFFERENCES IN THE LOWEST THREE KILOMETERS OF THE ATMOSPHERE

Francis J. Merceret* and Jennifer G. Ward
NASA, Kennedy Space Center, Florida

1. INTRODUCTION

Spatial properties of wind differences are important to launch and landing operations because wind hazards and wind effects on vehicle loads and navigation are assessed based on measurements by instruments located some distance from the planned flight track of the vehicle. When the measurements are near operational go/no-go thresholds ("redlines"), the question arises as to the likelihood that the vehicle will experience winds above those thresholds. The answer requires knowledge of the temporal and spatial properties of the wind field.

Temporal differences have been extensively explored in studies reported in the literature, especially for the mid and upper troposphere in the region of maximum dynamic pressure on ascent (*See, e.g.,* Merceret, 1997; Merceret, 2000 and Spiekerman *et al.*, 2000). Spatial differences have not been as well examined because such research requires a network of wind sensors with the appropriate spacing and such networks are rare. Wind tower measurements are limited to the lowest hundred meters or less and balloons provide small sample sizes at uncontrollable locations as they slowly ascend following the wind. The Eastern Range (ER) network of five 915 MHz boundary layer wind profilers provided a unique opportunity to examine the spatial variability of winds in the Shuttle roll maneuver region below 3 km altitude as requested by the Shuttle program.

This paper presents temporal and spatial analyses of wind profile differences. The temporal analyses examine the differences between profiles separated in time at each profiler. The spatial analyses examine the differences between simultaneous profiles at pairs of wind profilers. Five profilers allow for ten distinct pair combinations spaced from 8.5 to 31 km apart. A research grade data set was prepared covering the period from November 1999 through August 2001. Extensive automated and manual quality control was applied (Lambert *et al.*, 2003). Complete profiles of wind speed and direction were available at 15 minute intervals covering the altitude range from about 100 to 3000 meters in "range gates" about 100m thick.

The analyses were conducted using three methods: structure functions (SF), correlation analysis and spectral analysis. Separate results are presented for the summer (June through September) and winter (December through March) seasons as defined for ER wind climatology by the Space Shuttle program. The results are also stratified by altitude and time of day.

2. PROFILER GEOMETRY

To generate temporal SF or coherence, a single instrument may be used, but to generate spatial SF or coherence, multiple instruments are required to produce differing distances between measurements. The Eastern Range network of five 915 MHz boundary layer profilers shown in figure 1 permits ten distinct pairs of measurements. These enable generation of SF and coherences at ten separations as shown in table 1. In addition,

Profiler Pair	Distance (km)	Bearing (deg)
2,3	8.45	238
3,5	14.42	243
3,4	15.07	339
2,4	15.86	307
1,3	16.03	328
1,2	18.09	356
4,5	21.93	200
1,5	22.46	288
2,5	22.85	241
1,4	30.97	333

Table 1. Distance and bearing between pairs of instruments in the ER boundary layer profiler network.

Corresponding author address: Francis J. Merceret, NASA YA-D, Kennedy Space Center, FL 32899; email: francis.j.merceret@nasa.gov

the varying directions between the members of each pair permits examination of the effects of the alignment of the separation vector with the wind direction.

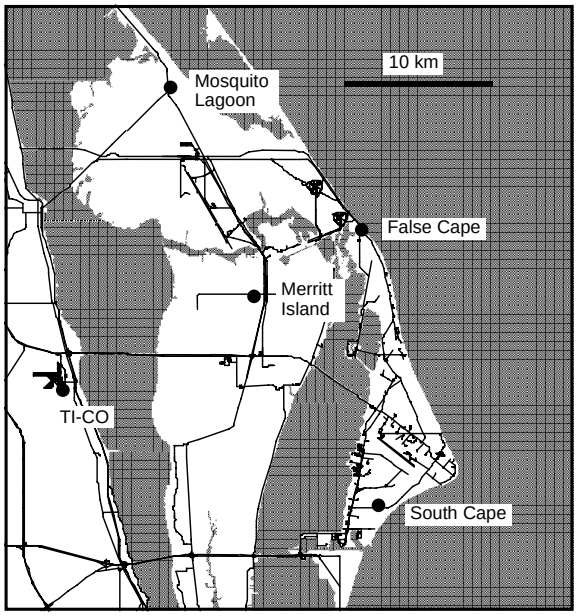

Figure 1. Locations of the five boundary layer profilers used in this study. The profilers are numbered as follows: South Cape = 1, False Cape = 2, Merritt Island = 3, Mosquito Lagoon = 4 and TICO = 5.

3. DATA STRATIFICATION

3.1 *Temporal Stratification*

To examine seasonal effects, the data were divided into winter (Julian days 335 - 091) and summer (days 153 -274) seasons. To examine diurnal effects, the seasonal data were further subdivided into day and night categories as follows:

- Summer day (13 – 22 Z)
- Summer night (2 – 7 Z)
- Winter day (14 – 19 Z)
- Winter night (2 – 9 Z).

Times denote the end of the hour.

3.2 *Altitude Stratification*

For this analysis, data were available from the lowest thirty range gates of the profilers. To retain the ability to examine the effects of altitude while reducing the labor and increasing the sample size, the analysis combined sets of three adjacent gates into "levels". The nominal height of each level is shown in table 2.

Level #	Bottom (m)	Center (m)	Top (m)
1	430	530	640
2	740	840	940
3	1040	1140	1240
4	1340	1440	1540
5	1650	1750	1850
6	1950	2050	2150
7	2250	2350	2450
8	2550	2660	2760
9	2860	2960	3060

Table 2. Altitudes of analysis levels

3.3 *Wind Direction Stratification*

The spatial structure functions and correlations were computed for all cases regardless of wind direction, along wind cases and crosswind cases. Along wind and cross wind were defined by the angle between the wind vector and the separation vector being within 20 degrees of parallel and perpendicular respectively. The power spectra and coherences were not stratified by wind direction because the sample size was too small.

4. STRUCTURE FUNCTIONS

4.1 *Background*

Structure functions are the mean square differences between two measurements separated either in time or space. They provide a measure of the magnitude of the difference between the measurements as a function of their temporal or spatial separation. Analytically, the temporal and spatial structure functions for a quantity, q, are given by

$SFTq\ (\tau) = < (q(t+\tau) - q(t))^2 >$ and

$SFSq\ (\underline{\mathbf{r}}) = <(q(\underline{\mathbf{x}}+\underline{\mathbf{r}}) - q(\underline{\mathbf{x}}))^2>$

where the pointed brackets denote the ensemble average. For our study the vector nature of the spatial separation, $\underline{\mathbf{r}}$, was accounted for by doing three separate calculations. The first ignored the direction entirely, and used only the magnitude, r, of the separation. The other two restricted analysis

respectively to along wind and cross wind separations.

SF are frequently computed for wind speed, temperature, or relative humidity. For further discussion, see Stull, 1988. SF are also used extensively by radar and optical remote sensing meteorologists where the variable q is the microwave or optical index of refraction (references omitted). For our study, q is the windspeed.

At temporal or spatial separations in the inertial subrange of the neutral atmosphere, SF typically obey a power law with an exponent near 2/3. At large separations, the SF asymptotically become constant because the spatially or temporally separated variables have become completely independent and further separation cannot further decorrelate them. Of course, at zero separation the SF are identically zero.

4.2 *Method of Computation*

For each calendar day in the period of record the daily structure function of wind speed (subject to the stratifications described in Section 3) was computed for time lags of 0.25, 055, 1 and 2 hours and for the spatial separations given in Table 1. The daily structure function is the structure function defined by Section 4.1 above where the average (<x>) is taken over the calendar day beginning at 00Z and ending at 24Z. These daily structure functions were then summed over the number of days in the record and the sum divided by the number of days in the sum to produce the seasonally averaged results presented here.

4.3 *Temporal Results*

The summer daytime results are presented in tables 3a and 3b. The least squares parameters are for a fit of the form SF = $A\tau^B$ with r^2 being the correlation coefficient for the regression (not to be confused with the same symbol when used to represent spatial separation distance).

	All Profilers Temporal Lag (hours)			
Level	0.25	0.5	1	2
Level 1	0.898	1.299	2.130	3.809
Level 2	0.901	1.246	1.893	3.164
Level 3	0.912	1.238	1.817	2.888
Level 4	0.981	1.337	1.940	3.042
Level 5	1.053	1.428	2.055	3.081
Level 6	1.080	1.479	2.112	3.313
Level 7	1.129	1.561	2.194	3.499
Level 8	1.217	1.711	2.387	3.734
Level 9	1.304	1.857	2.674	4.222

Table 3a. Temporal structure functions ($m^2 s^{-2}$) for summer days as a function of level.

The power law fit is excellent although the high r^2 value can be misleading with only four (x,y) pairs in the fit. The value of the exponent B is smaller than 2/3 except at the first two levels where the differences is not statistically significant at the 10% level. In fact, the value B = 0.575 fits all levels except level 1 and level 5 at the 10% level of significance.

	Power Law Fit		
Level	A	B	r^2
Level 1	2.2330	0.6967	0.9904
Level 2	1.9853	0.6040	0.9899
Level 3	1.8906	0.5542	0.9916
Level 4	2.0137	0.5435	0.9931
Level 5	2.1014	0.5172	0.9961
Level 6	2.2021	0.5365	0.9932
Level 7	2.3115	0.5387	0.9919
Level 8	2.4969	0.5333	0.9948
Level 9	2.7774	0.5611	0.9961

Table 3b. Least squares parameters fitting the results in Table 3a to the form SF = $A\tau^B$.

Tables 4a and 4b present the summer nighttime results. They are similar although the value of B in table 4b in the lowest levels is significantly larger than for the daytime case. B = 0.600 fits levels 5 through 9 at the 10% level of significance. The values of B for level1 and level 2 are each unique at the 10% level of significance.

	All Profilers Temporal Lag (hours)			
Level	0.25	0.5	1	2
Level 1	0.572	1.021	1.849	3.075
Level 2	0.633	1.059	1.757	3.001
Level 3	0.734	1.136	1.836	2.975
Level 4	0.824	1.229	1.959	3.037
Level 5	0.918	1.360	2.067	3.134
Level 6	0.987	1.525	2.243	3.277
Level 7	0.999	1.415	2.200	3.264
Level 8	1.159	1.519	2.303	3.546
Level 9	1.157	1.586	2.358	3.602

Table 4a. Temporal structure functions ($m^2 s^{-2}$) for summer nights as a function of level.

The corresponding winter data are presented in Tables 5a through 6b. Again, the fits are excellent and, again, the lowest levels have larger exponents at night. The winter SF appear to have larger exponents both day and night than the corresponding summer SF. The winter daytime fits for the lowest six levels are consistent with B = 0.740 at the 10% level, but the higher gates are significantly smaller. The winter night fits are consistent with B = 0.760 at the 10% level except for the lowest level and the highest two levels.

	Power Law Fit		
Level	A	B	r^2
Level 1	1.7896	0.8136	0.9989
Level 2	1.7761	0.7466	0.9999
Level 3	1.8459	0.6750	0.9994
Level 4	1.9503	0.6318	0.9991
Level 5	2.0703	0.5918	0.9998
Level 6	2.2260	0.5750	0.9989
Level 7	2.1794	0.5761	0.9981
Level 8	2.3513	0.5440	0.9898
Level 9	2.4031	0.5487	0.9958

Table 4b. Least squares parameters fitting the results in Table 4a to the form $SF = A\tau^B$.

	All Profilers Temporal Lag (hours)			
Level	0.25	0.5	1	2
Level 1	0.946	1.448	2.337	4.167
Level 2	0.872	1.361	2.298	3.983
Level 3	0.903	1.387	2.340	3.961
Level 4	0.937	1.456	2.543	4.309
Level 5	1.043	1.709	2.940	5.107
Level 6	1.125	1.706	2.737	4.923
Level 7	1.203	1.826	2.999	4.713
Level 8	1.385	2.220	3.313	4.797
Level 9	1.509	2.396	3.521	5.134

Table 5a. Temporal structure functions ($m^2 s^{-2}$) for winter days as a function of level.

	Power Law Fit		
Level	A	B	r^2
Level 1	2.4449	0.7108	0.9951
Level 2	2.3405	0.7330	0.9978
Level 3	2.3652	0.7154	0.9978
Level 4	2.5419	0.7408	0.9978
Level 5	2.9658	0.7658	0.9993
Level 6	2.8813	0.7071	0.9938
Level 7	2.9699	0.6626	0.9990
Level 8	3.2499	0.5954	0.9969
Level 9	3.4830	0.5855	0.9975

Table 5b. Least squares parameters fitting the results in Table 5a to the form $SF = A\tau^B$.

	All Profilers Temporal Lag (hours)			
Level	0.25	0.5	1	2
Level 1	0.622	1.032	1.840	3.568
Level 2	0.688	1.125	2.030	3.763
Level 3	0.757	1.249	2.245	3.816
Level 4	0.845	1.349	2.352	3.941
Level 5	0.959	1.521	2.629	4.300
Level 6	1.037	1.581	2.744	4.788
Level 7	1.125	1.712	2.735	5.491
Level 8	1.274	2.063	3.069	4.942
Level 9	1.325	2.363	3.539	5.171

Table6a. Temporal structure functions ($m^2 s^{-2}$) for winter nights as a function of level.

	Power Law Fit		
Level	A	B	r^2
Level 1	1.9166	0.8395	0.9964
Level 2	2.0723	0.8206	0.9974
Level 3	2.2143	0.7847	0.9992
Level 4	2.3354	0.7467	0.9990
Level 5	2.5938	0.7284	0.9990
Level 6	2.7857	0.7416	0.9960
Level 7	3.0114	0.7537	0.9850
Level 8	3.1411	0.6440	0.9986
Level 9	3.4436	0.6476	0.9891

Table 6b. Least squares parameters fitting the results in Table 6a to the form $SF = A\tau^B$.

The temporal structure functions all follow the expected pattern. They increase systematically with time lag following a power law, and they also increase with altitude consistent with the shape of boundary layer wind profiles.

4.4 *Spatial Results*

Unlike the raw temporal SF, the raw spatial SF behave badly. Not only do they not fit a power law well, they do not even increase monotonically with separation distance. There are at least two reasons for this, one somewhat expected and the other completely unanticipated. These will be discussed below.

The easiest way to get an immediate appreciation for the difference between the spatial and temporal SF is to look at figure 2. Figure 2 and table 7 present the summer daytime raw spatial structure functions.

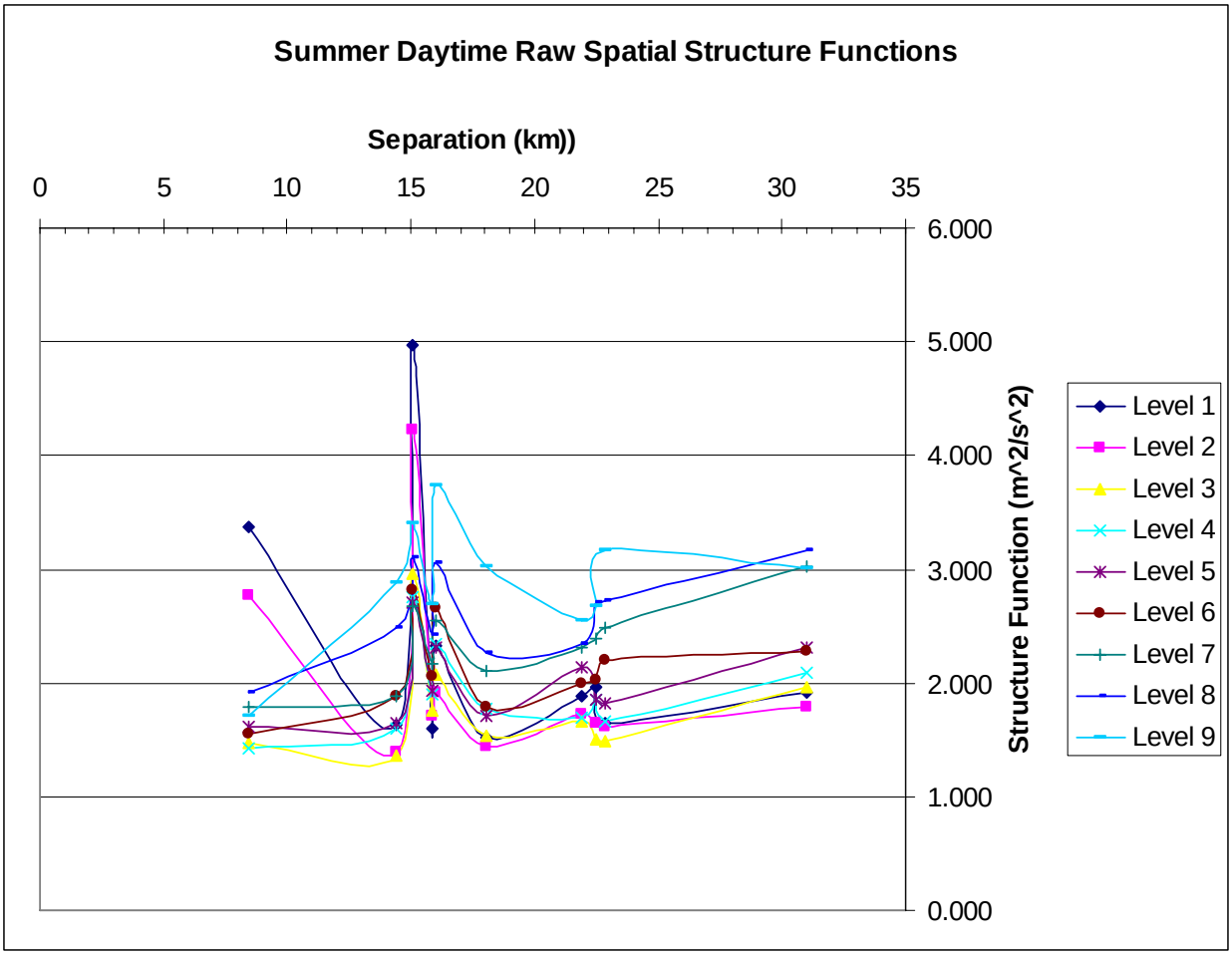

Figure 2. Raw spatial structure functions (m^2 s^{-2}) for summer days as a function of level.

Level\Lag	8.45	14.42	15.07	15.86	16.03	18.08	21.93	22.46	22.85	30.97
Level 1	3.374	1.637	4.976	1.600	2.333	1.5150	1.8910	1.9590	1.643	1.916
Level 2	2.777	1.391	4.220	1.704	1.91	1.4340	1.7290	1.6430	1.612	1.782
Level 3	1.468	1.367	2.966	1.760	2.068	1.5280	1.6640	1.5030	1.491	1.959
Level 4	1.421	1.603	2.752	1.902	2.35	1.7670	1.6960	1.8580	1.663	2.093
Level 5	1.612	1.643	2.713	1.929	2.31	1.7020	2.1350	1.8550	1.814	2.308
Level 6	1.549	1.881	2.818	2.060	2.662	1.7940	1.9930	2.0270	2.207	2.287
Level 7	1.794	1.877	2.677	2.176	2.541	2.0980	2.3070	2.3930	2.483	3.024
Level 8	1.909	2.493	3.096	2.420	3.054	2.2610	2.3500	2.7000	2.722	3.163
Level 9	1.715	2.884	3.410	2.686	3.741	3.0270	2.5430	2.6690	3.17	3.013

Table 7. Spatial structure functions (m^2 s^{-2}) for summer days as a function of level and spatial separation (Lag) in km.

One reason that a power law relation does not fit the observations would be that the separation between profilers is so large that the SF have reached their asymptotic limit. This hypothesis is consistent with wind tower measurements by Merceret (1995) who found that at a height of 30 feet, the spatial structure functions reached their asymptotic limit at spacings as small as 200 feet and no larger than 3000 feet (1 km).

The smallest spacing in the RWP array is more than eight time larger than the largest spacing found to be asymptotic in the tower measurements. In this case, however, we would not expect to see peaks and dips much larger than the sampling variation in the plots.

There is, however, another factor that was completely unexpected. Detailed examination of the tabular data indicated that the largest deviations from either power law or asymptotic behavior all seemed to involve pairs in which one of the profilers was RWP 3. If RWP 3 is removed from figure 2 then figure 3 is the result.

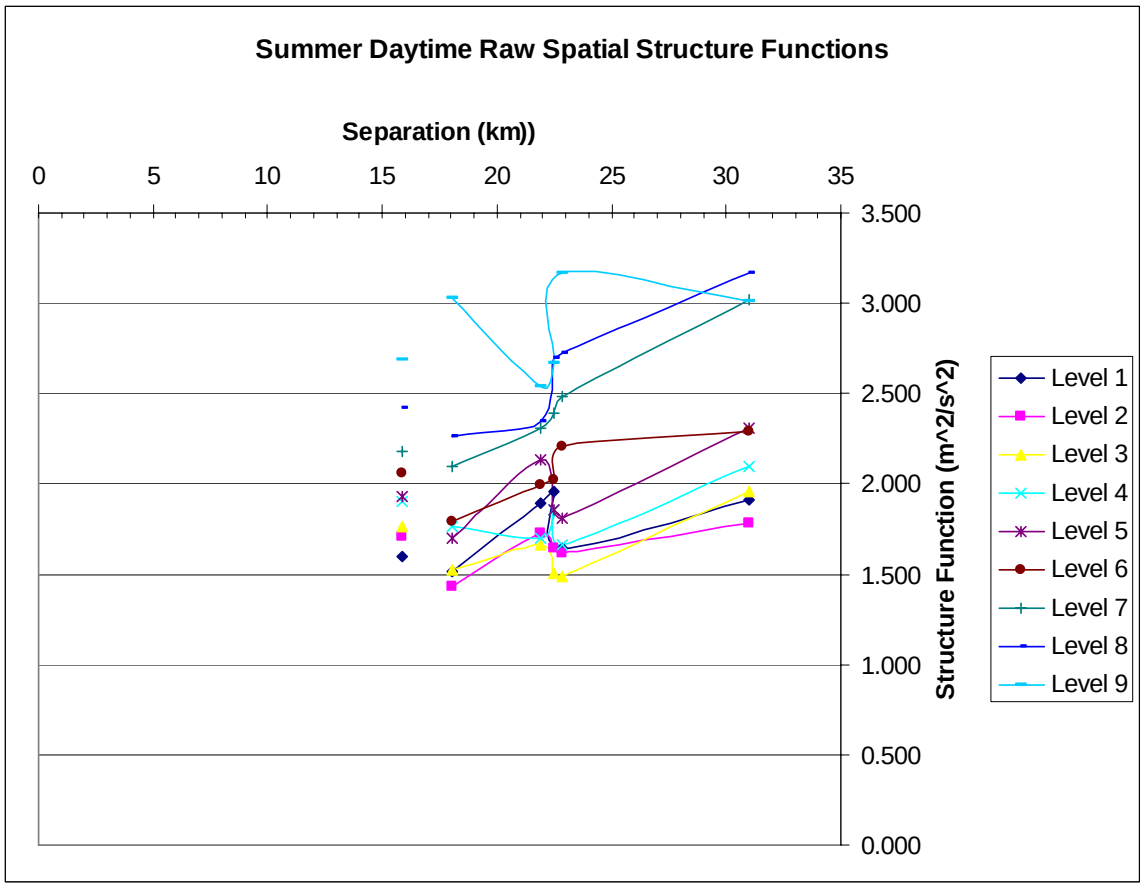

Figure 3. Same as figure 2 with RWP 3 removed and scale expanded.

	All Winds Spatial Lag (kilometers)								
Level\lLag	15.86	18.08	21.93	22.46	22.85	30.97	A	B	r^2
Level 1	1.6	1.515	1.891	1.959	1.643	1.916	0.6220	0.3361	0.4952
Level 2	1.704	1.434	1.729	1.643	1.612	1.782	1.0069	0.1602	0.2288
Level 3	1.76	1.528	1.664	1.503	1.491	1.959	0.9544	0.1769	0.1401
Level 4	1.902	1.767	1.696	1.858	1.663	2.093	1.1862	0.1402	0.1435
Level 5	1.929	1.702	2.135	1.855	1.814	2.308	0.7303	0.3194	0.4242
Level 6	2.06	1.794	1.993	2.027	2.207	2.287	0.9593	0.2482	0.4465
Level 7	2.176	2.098	2.307	2.393	2.483	3.024	0.4714	0.5296	0.8761
Level 8	2.42	2.261	2.35	2.7	2.722	3.163	0.6324	0.4587	0.7185
Level 9	2.686	3.027	2.543	2.669	3.17	3.013	2.0161	0.1119	0.0844

Table 8. Same as table 7 with RWP 3 removed and with corresponding parameters for the power law least squares fit added.

These plots appear to have some slope to them and the large peaks and dips are gone. The traces are still nowhere as neat as those for the temporal SF and the power fits are unimpressive, especially with only four (x,y) pairs, as may be seen from the r^2 values in table 8. This suggests that the separation is probably asymptotic with regard to the small scale turbulence normally associated with structure function analysis, but not with respect to larger scale driving functions such as sea breezes which may account for the residual slope.

Tables 9, 10 and 11 respectively present the raw spatial structure functions for summer nights, winter days and winter nights. Distances involving RWP 3 are highlighted.

Level\Lag	8.45	14.42	15.07	15.86	16.03	18.08	21.93	22.46	22.85	30.97
Level 1	1.241	1.268	1.887	1.137	2.174	1.1140	2.2400	1.8890	1.864	1.905
Level 2	1.154	1.162	1.542	1.140	2.022	1.2770	1.9510	1.6810	1.623	2.146
Level 3	1.325	1.407	1.740	1.376	1.837	1.4520	2.1600	1.8150	1.941	2.254
Level 4	1.149	1.355	1.655	1.546	1.601	1.6390	2.4610	1.8940	2.027	2.506
Level 5	1.292	1.949	1.995	1.662	1.79	1.6590	2.3010	2.4650	2.383	2.527
Level 6	1.113	2.230	2.144	1.978	1.816	1.6360	2.2840	1.9900	2.224	2.431
Level 7	1.298	1.524	2.110	1.688	1.89	1.9510	1.9800	1.9270	1.823	2.206
Level 8	1.644	1.402	2.567	2.091	2.284	2.2410	1.8550	1.9950	1.938	2.846
Level 9	1.396	1.907	2.830	2.343	2.484	2.2730	2.1230	2.4780	1.934	2.603

Table 9. Spatial structure functions (m^2 s^{-2}) for summer nights as a function of level and separation (lag).

Level\Lag	8.45	14.42	15.07	15.86	16.03	18.08	21.93	22.46	22.85	30.97
Level 1	1.821	2.024	3.164	1.775	2.551	1.6060	2.3140	2.9060	3.052	2.479
Level 2	1.834	1.481	3.137	1.483	2.932	1.5560	1.8180	2.1940	1.851	2.248
Level 3	1.425	1.472	3.038	1.416	3.451	1.7370	1.7390	2.4200	1.856	2.601
Level 4	1.392	1.149	2.831	1.510	4.739	1.5110	1.6000	2.3090	1.693	2.625
Level 5	1.424	1.327	3.883	1.771	5.176	1.6720	1.9860	3.1280	2.245	2.992
Level 6	1.170	1.359	4.419	1.614	4.681	1.7150	1.8740	2.4560	1.823	2.995
Level 7	1.095	1.651	5.538	1.590	5.455	2.1670	2.3090	2.8120	1.768	3.65
Level 8	1.077	1.753	2.542	2.069	7.529	1.9190	2.4620	2.8000	2.199	4.417
Level 9	1.473	2.268	2.768	2.254	3.02	2.3830	2.1070	3.0990	3.033	4.617

Table 10. Same as Table 9 for winter days.

Level\Lag	8.45	14.42	15.07	15.86	16.03	18.08	21.93	22.46	22.85	30.97
Level 1	2.198	1.293	2.619	1.392	1.98	1.3990	2.6110	1.5620	2.882	2.027
Level 2	2.148	1.437	3.159	1.291	3.081	1.5900	2.7450	1.9950	2.755	2.111
Level 3	3.017	1.479	4.628	1.510	5.309	1.5510	1.9760	2.0750	2.246	2.462
Level 4	6.832	1.289	4.532	1.523	4.013	1.7660	1.8390	2.0340	2.36	2.788
Level 5	5.049	1.327	6.474	1.759	5.895	1.9780	2.4790	2.6350	2.63	3.191
Level 6	9.296	1.418	9.890	1.731	11.075	2.1850	1.7870	2.9490	3.158	4.422
Level 7	7.052	1.370	9.650	1.967	8.622	2.1290	1.9950	3.2430	2.348	4.187
Level 8	6.919	1.439	14.478	2.089	12.223	2.5770	1.7470	2.9960	1.732	4.419
Level 9	9.798	1.642	2.963	2.626	9.97	2.8580	2.4700	2.6300	2.731	4.566

Table 11. Same as Table 9 for winter nights.

The foregoing results are for all winds regardless of direction. In general, the along wind and cross wind SF do not differ significantly from the all-wind SF. There are two exceptions.

In many cases, SF involving RWP 3 show a directional dependence, and the summer daytime crosswind SF differ somewhat from the all-wind SF. To quantify the differences in a consistent manner, let's define the fractional absolute difference, F, for the cross or along wind case with respect to the all-wind case by

Fx = ABS [(SFx – SFall)/SFall)]

where x = along or cross. If F does not exceed 0.5, then the RMS difference between the first profiler and the second does not differ more than 22 % depending on direction. The RMS differences are on the order of 1 to 2 m s^{-1} so 22% is within the 1 m s^{-1} RMS error of measurement of the profilers. In table 12 below, values of F > 0.5 are printed in red. Distances involving RWP3 are highlighted in yellow.

	(Cross - All) Winds Spatial Lag (kilometers)									
Level	8.45	14.42	15.07	15.86	16.03	18.08	21.93	22.46	22.85	30.97
1	0.093	0.697	0.374	0.178	0.214	0.136	0.451	0.090	0.417	0.224
2	0.077	0.454	0.471	0.080	0.289	0.037	0.208	0.162	0.293	0.155
3	0.226	0.007	0.398	0.032	0.314	0.123	0.198	0.453	0.158	0.033
4	0.024	0.410	0.473	0.140	0.611	0.050	0.094	0.162	0.058	0.222
5	0.098	0.102	0.634	0.180	0.623	0.009	0.015	0.349	0.229	0.273
6	0.235	0.073	0.600	0.282	0.551	0.011	0.053	0.992	0.180	0.192
7	0.292	0.402	0.599	0.193	0.599	0.142	0.313	0.299	0.295	0.006
8	0.268	0.453	0.105	0.040	0.616	0.278	0.303	0.703	0.382	0.071
9	0.701	1.764	0.241	0.214	0.156	0.145	0.125	0.151	0.506	0.043

Table 12. Fcrosswind (see text for definition) for winter days. Values greater than 0.5 are in red font. Distances involving RWP3 are highlighted in yellow.

Table 12 shows F for crosswinds in the winter during daytime, a typical case. Except for separations involving RWP 3 near 15 km separation, most values of F are below 0.5, but about a third of the RWP3 cases are above 0.5.

The best case was summer nighttime along wind where only three of 90 entries in the corresponding table (not shown) are red. The worst cases were crosswinds, summer daytime and winter nighttime. The summer daytime crosswind F values exceeded 0.5 in 23 of the 90 entries, seven of which involved RWP3. The winter nighttime crosswind F values exceeded 0.5 in 28 of the 90 entries, but 23 of these involved RWP3.

The results presented above clearly suggest that there is something unusual about spatial SF involving RWP3 that deserves discussion.

4.5 *Discussion*

The temporal SF are remarkably unremarkable. As noted above, they all follow the expected pattern. They increase systematically with time lag following a power law, and they also increase with altitude consistent with the shape of boundary layer wind profiles. The temporal SF for the five individual RWP were examined separately and RWP3 shows no anomalous behavior in the time domain.

The spatial SF clearly suggest that the RWPs are too far apart for the oft-cited power law to apply. The separation exceeds the asymptotic distance of about 1 km found near the surface by Merceret, 1995 by an order of magnitude. This is probably large enough that some variation with distance due to large scale effects occurs.

The uniqueness of RWP3 in the spatial domain initially seemed so inexplicable that the authors retested the software and revalidated the data files to be sure there was no error. Detailed consideration of the local geography

and the locations of the profilers suggested a possible contributor to the phenomenon.

Examination of high-resolution maps provided by the KSC planning department showed that RWP 3 (Merritt Island) was sited differently than the other profilers in two ways that could result in systematic differences in the wind speeds measured at a given altitude. First, as may be seen from figure 4, all of the 915 MHz profilers except RWP 3 have significant bodies of water immediately to their east. RWP 1 (South Cape) and 2 (False Cape) are on the Atlantic Ocean. RWP 5 (TICO) is on the Indian River and RWP 4 (Mosquito Lagoon) abuts Mosquito Lagoon which, except for some insignificant sand bars, is the shore of the Atlantic Ocean. RWP is 5 to 8 km inland in all directions including to the east.

The other difference is that RWP 3 is located near the KSC industrial area and has buildings and tall trees in most directions except to the northwest where it has one of the worlds largest concrete runways. RWP 1,2 and 4 are located in predominantly rural areas on coastal terrain where large structures and tall trees are farther away and occupy only a limited range of directions. RWP 5 is situated similar to RWP 3 from westerly azimuths between about 160 and 020 degrees, but like RWP 1, 2 and 4 for azimuths between 020 and 160.

Surface properties can affect wind profiles in several ways. Surface roughness impacts the profile through a parameter called the "roughness length" that determines the vertical scale of variation of the mean wind for a given turbulence level. The classical "logarithmic profile" for neutral boundary layer winds is given by

$$\langle WS \rangle = (u^*/k) \ln (z/z_o)$$

Where u^*, the "friction velocity", is a measure of turbulence intensity, z is height above the surface, k is Kolmogorov's constant ~ 0.4, and z_o is the roughness length discussed above (See Stull cited above for details). If the same large scale wind forcing and overall turbulence level affects all five profilers, but the roughness length at RWP3 is different, its vertical wind profiles will differ from the others. This vertical rescaling will not significantly affect the temporal behavior at RWP 3 unless there are large vertical gradients in the temporal structure functions, but there aren't. Roughness lengths over water are typical an order of magnitude or more smaller than those over land, and those in forested or built up areas are larger than those in rural, shrubbed areas. It is highly likely that z_o at RWP3 is larger than at any of the other RWP for most wind directions except for westerly component winds at RWP5.

Surface thermal properties can also affect the vertical structure of boundary layer profiles through their effect on low level stability. The logarithmic profile works well in near neutral conditions, but in non-neutral conditions the equation has additional terms involving stability parameters (See Stull above). The surface temperature, soil properties or sea state all affect heat and moisture transport through the bottom boundary of the atmosphere, thus strongly affecting stability and the shape of the profile. Obviously a land-locked somewhat built-up area like that around RWP3 will have differing nearby surface thermal and moisture characteristics than the seashore.

The summertime data show that the RWP 3 anomaly is worse in the daytime than at night. This is consistent with hot summer days under intense direct insolation with enough low-level humidity at night to prevent major radiational cooling of the surface. The wintertime anomaly is much worse at night, consistent with reduced daytime heating but major radiational cooling under clear skies and dry conditions at night.

Differences in the surface properties affect the vertical structure of the profiles much more than the temporal structure. Since the spatial structure functions are computed by comparing profilers at the same height, alterations in the shape of one profile of the pair due to differing stability and roughness could alter the spatial structure function significantly without significant alteration in the temporal SF at either profiler of the pair. The data suggest this as the most likely cause of the RWP3 anomaly.

5. CORRELATION ANALYSIS

5.1 *Method of computation*

Time lagged autocorrelations and cross correlations for profiler pairs were computed directly for lags of -120 to 120 minutes in 15

minute increments for each seasonal and time of day stratification. In addition, cross correlations were computed for pairs of profilers where the data were limited to those satisfying the along wind or cross wind constraint.

The results reported in this preprint do not include those using the wind direction stratifications for several reasons. First, a preliminary examination of the data did not reveal any obvious or systematic differences between the along wind and cross wind cases which both looked very similar to the "all winds" data. Second, the sample sizes were quite small given the 20 degree direction constraint, so the sampling variability was relatively large and suggested caution in interpreting possible signals. Third, there was not time prior to the due date of this manuscript to devote the necessary effort to going beyond the preliminary examination. If additional examination reveals useful information prior to the presentation at the conference, the poster will include that information.

5.2 *Autocorrelation Results*

The autocorrelations for each of the five profilers were similar but not identical for any given season, time and level. Figure 4 shows the autocorrelations for all five profilers at level 3 for summer days.

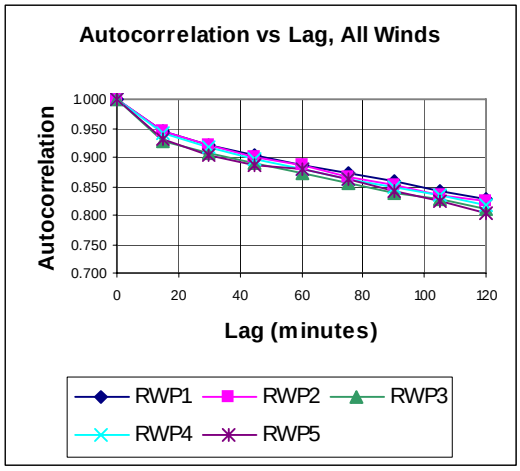

Figure 3. Autocorrelations for summer days at level 3.

The shape of the autocorrelation functions could not be fit to a first order autoregressive moving average process because the rate of decline of the autocorrelation with lag decreased with lag rather than remaining constant. In a few cases, there were significant differences between several of the profilers. These cases are being examined to see if these differences are meaningful. An example is given in Figure 5.

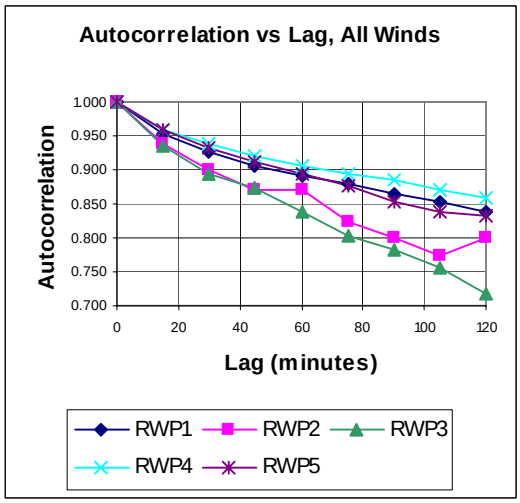

Figure 5. Autocorrelations for summer nights at level 7.

This "grouping" of profilers (*e.g.* RWP 2 and 3 vs 1, 4 and 5 in Fig. 5) appears mostly at higher altitudes where the sample sizes are smaller and is not consistent enough to warrant further discussion without additional analysis.

The autocorrelations do not appear to vary significantly with height. Figure 6 shows

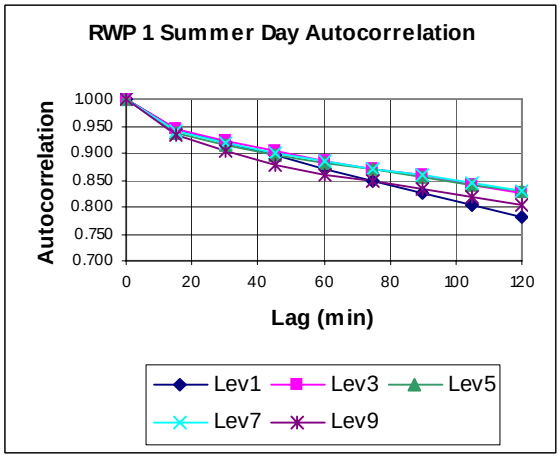

Figure 6. Autocorrelations as a function of level for RWP1 in the summer daytime.

curves for each of the levels for RWP1 in the daytime during summer. The winter nighttime

curves (not shown) cluster even more tightly together.

On the other hand, there is a clear seasonal signature in the autocorrelation at all heights.

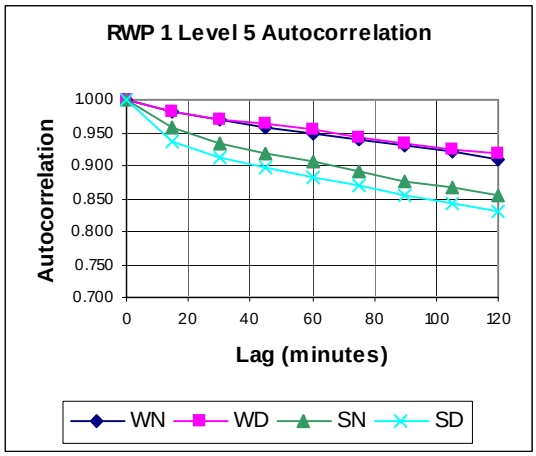

Figure 7. RWP1 Level 5 autocorrelation as a function of season and time of day.

The autocorrelations decrease more rapidly as a function of lag in the summer than in the winter. This is true at all levels for all profilers for both day and night. Figure 7 provides an example.

5.3 *Cross-correlation Results*

The cross correlations produced three interesting findings. Probably the most significant is that the cross correlations at all lags do not vary systematically with the separation distance between the profilers.

Figure 8 (which is typical) shows that while there is no systematic trend in the correlation with distance at any lag, at similar distances there can be significant differences that depend on the specific profiler pair selected. For example, the pair 3-4 at 15.07 km and the pair 1-3 at 16.03 km have a lower correlation than the pair 3-5 at 14.42 km and the pair 2-4 at 15.86 km. This may have to do with the siting of the specific profilers with respect to the complex land - water exposure at the Eastern Range. Additional discussion of this issue may appear in the poster.

The second finding is that there is a tendency for cross correlations to be larger at higher altitudes. Figure 9 is typical and Figure 10 shows the one exception, winter nights.

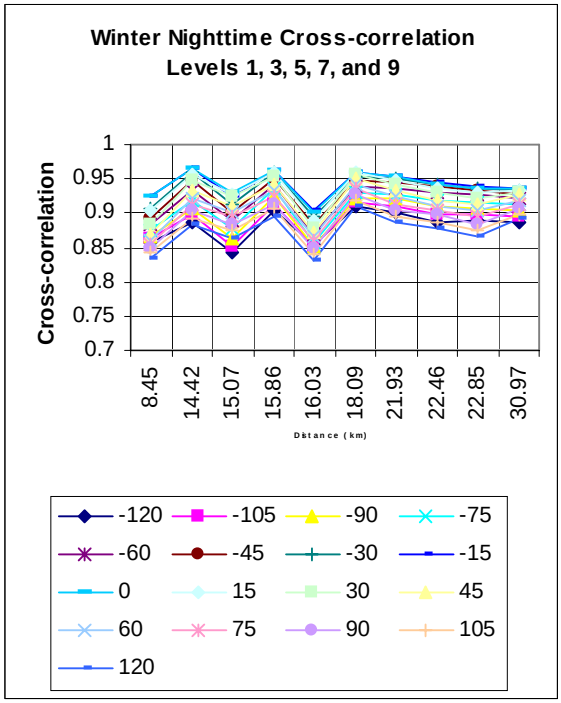

Figure 8. Cross correlation between profilers taken in pairs as a function of separation distance for all lags during the winter at night.

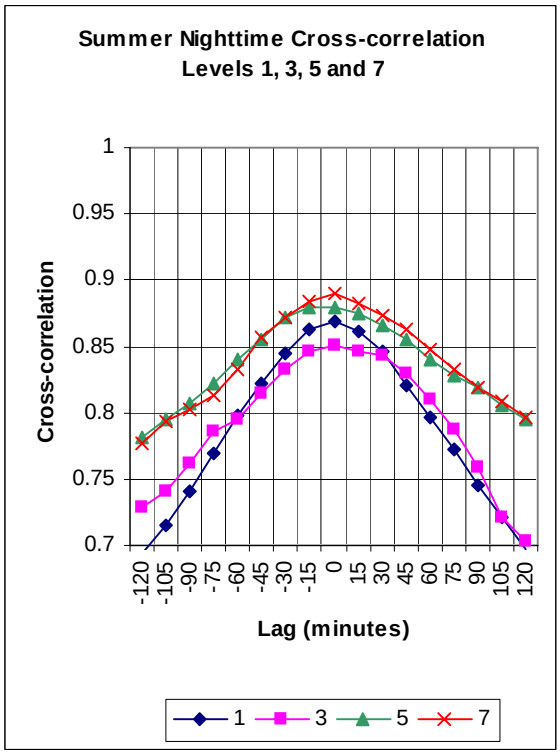

Figure 9. Average cross correlation for all profiler pairs for summer nights for levels 1

through 7. The sample size at level 9 was too small for a meaningful average to be computed.

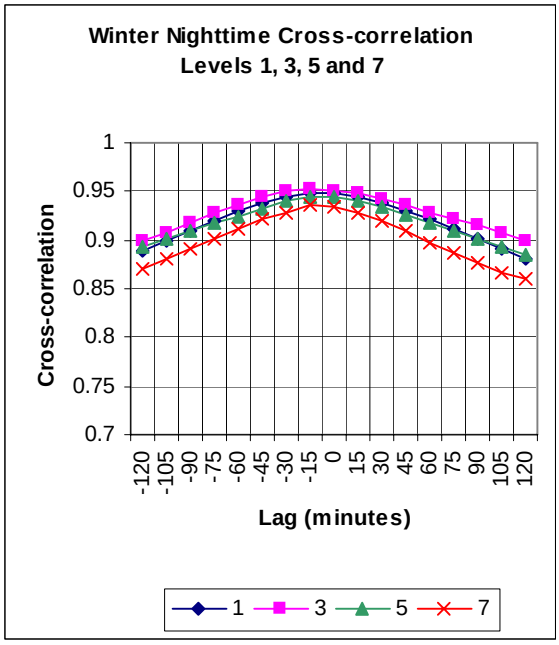

Figure 10. Average cross correlation for all profiler pairs for winter nights for levels 1 through 7. The sample size at level 9 was too small for a meaningful average to be computed.

The reason winter nights does not follow the same pattern as the other data is unknown at the time this manuscript is being prepared, but it may be due to the lessening of site-specific surface effects on the wind field with altitude.

The third finding is that regardless of time of day or altitude, the cross correlations are lower in the summer than in the winter. Figure 11 shows the cross correlations at level 5, representative of the data well above the surface, while Figure 12 shows them for the lowest level. The authors believe that this is because much of the variance in the summer wind field is due to local, thermally driven effects including active land, river and sea breezes and local convective activity. These phenomena are present during the winter, but their amplitude and frequency of occurrence are substantially smaller. This interpretation is consistent with winter days having an intermediate position in Figure 12, since central Florida is frequently warm enough during winter days for some of the summertime thermally driven effects to occur.

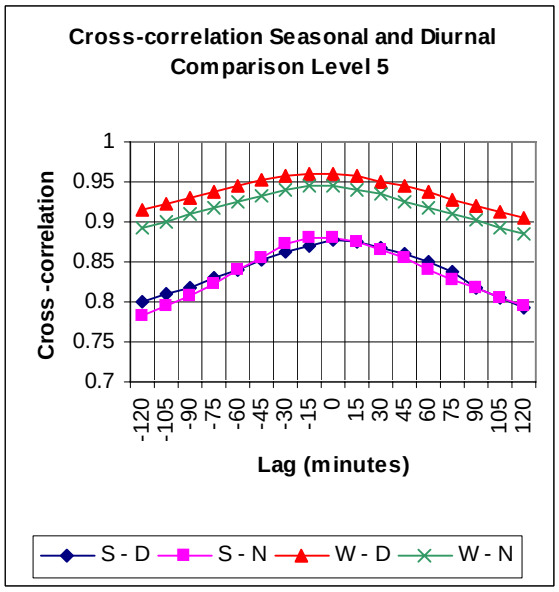

Figure 11. Average cross correlation for level 5 for the four seasonal/temporal stratifications. S-D denotes summer days, S-N denotes summer nights, and W-D and W-N respectively denote winter days and nights.

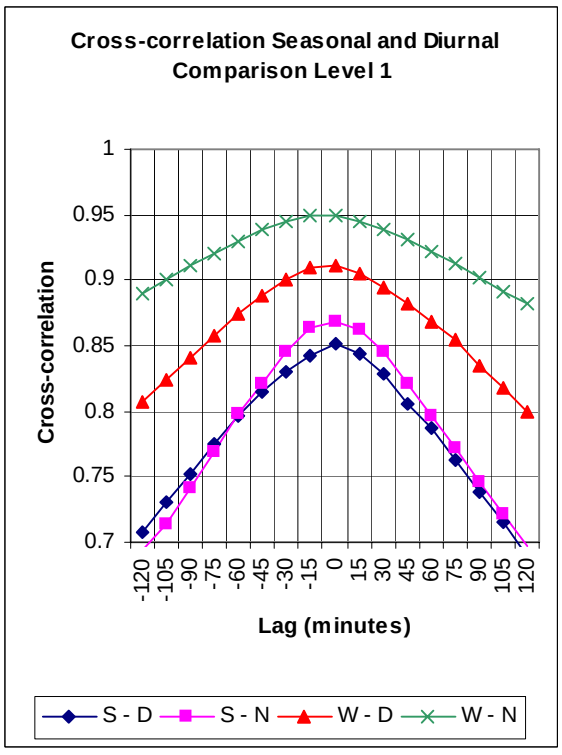

Figure 12. Same as Figure 11 for level 1.

5.4 *Discussion*

The finding that the cross correlations do not vary systematically with separation

between profilers is consistent with the results in section 4.4 for the spatial structure functions. It confirms that most of the wind variance is from scales of motion small enough in space and time that they are independent at separations of 8.5 km or more. The operational significance of this is discussed in section 7.1

The systematic variation of the cross correlations with height have not been explored in much detail here, but appear to be consistent with weakening local surface influence at higher altitudes.

The seasonal dependence of the cross correlations is similar to that of the autocorrelations reported in section 5.2, and both should be attributed to thermally driven local effects as described in the previous section.

6. SPECTRAL ANALYSIS

6.1 *Method of Computation*

Fast Fourier transforms (FFT) were taken on records of length 32 (8 hours) for pairs of profilers so that coherence could be calculated. The FFT software could not handle gaps in the data, so only 8 hour periods where there were no data missing for either profiler in a pair were used. The real and imaginary parts of the pair of FFTs were combined and averaged as required to form power and coherence spectra. Because the nighttime period during the summer and the daytime period during the winter were less than 8 hours long, spectral analysis was limited to winter nights and summer days. In cases where the number of individual FFTs averaged to produce a spectrum ("sample size") was less than 16, the results were not used. This assured that the sampling error of the spectral estimates was 25% or less.

6.2 *Power Spectra*

The power spectra showed conventional boundary layer power law behavior as shown in Figure 13 which is typical. The reference line in the figure has an inertial subrange slope of -5/3 for comparison. At the higher altitudes during the summer, the spectral slope flattened out at the higher frequencies, suggesting that the signal

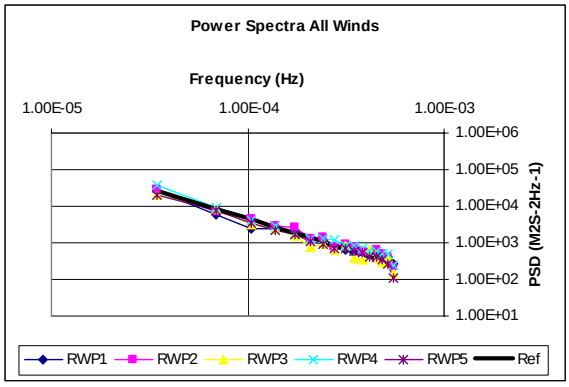

Figure 13. Power spectra for RWP 1 - 5 for the winter season nighttime at level 3.

was approaching the noise floor for that environment and altitude. An example is shown in Figure 14. Otherwise, there was no significant variation of the spectral characteristics with either season or altitude.

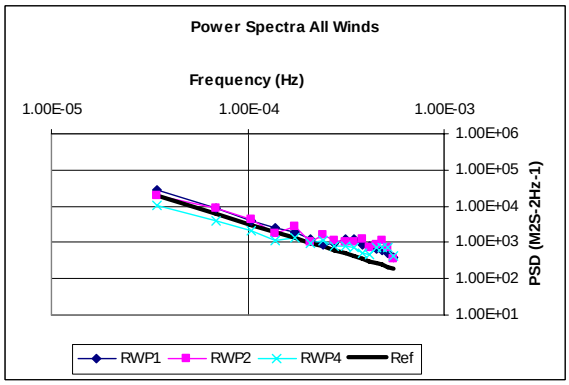

Figure 14. Power spectra for RWP 1, 2 and 4 for the summer season daytime at level 7 showing possible noise floor at frequencies above $3x10^{-4}$ Hz. Profilers 3 and 5 are not shown because they did not meet the minimum sample size criterion for spectral data.

6.3 *Coherence*

The coherence spectra depend on the separation between the profilers in each pair as expected, but they also depend on the season and the height. At the lowest level, the difference between seasons is not marked as may be seen by comparing Figure 15 with Figure 16. These two figures hint that the coherence at higher frequencies may be a bit higher in the summer, but the effect becomes more pronounced as one goes higher in altitude.

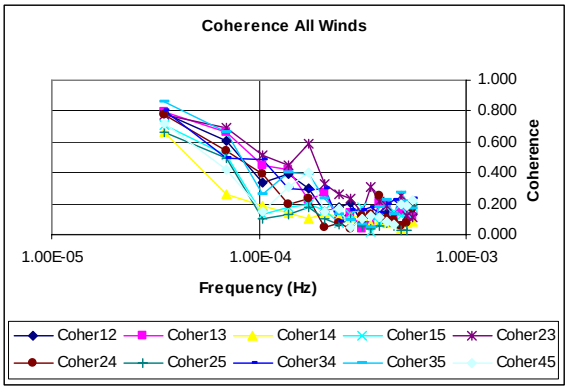

Figure 15. Coherence spectra for ten RWP pairs for the winter season nighttime at level 1.

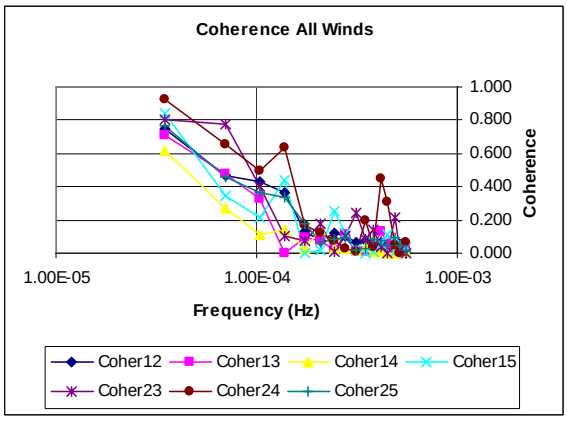

Figure 16. Coherence spectra for seven RWP pairs for the summer season daytime at level 1. The remaining pairs did not meet the required sample size criterion.

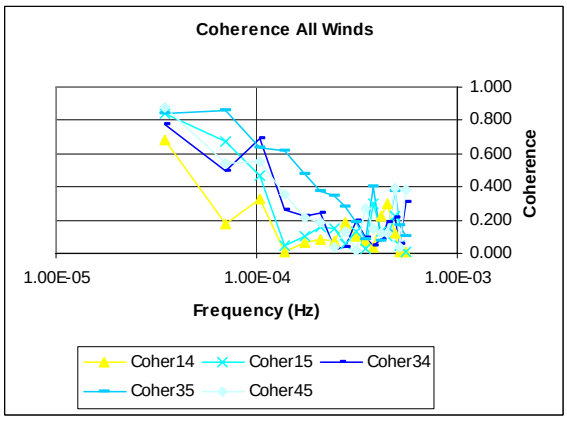

Figure 17. Coherence spectra for five RWP pairs for the winter season nighttime at level 7. The remaining pairs did not meet the required sample size criterion.

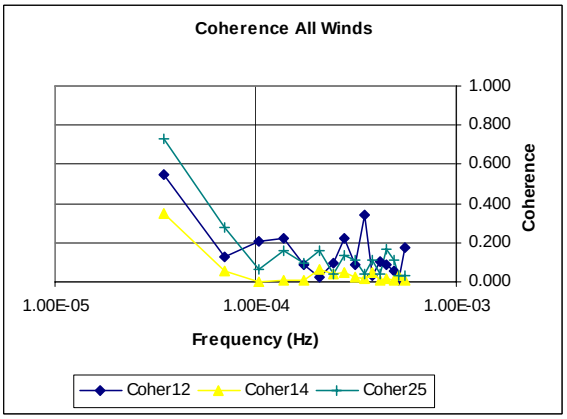

Figure 18. Coherence spectra for three RWP pairs for the summer season daytime at level 7. The remaining pairs did not meet the required sample size criterion.

Figures 17 and 18 respectively show the winter and summer coherences at level 7. The systematic lower coherence in the summer is easier to see in Figure 19 where the effects of varying spacing between profiler pairs (see below) has been eliminated by limiting the data to pairs with a spacing of 16 +/- 2 km, the mid range of available distances. A possible hypothesis is discussed below.

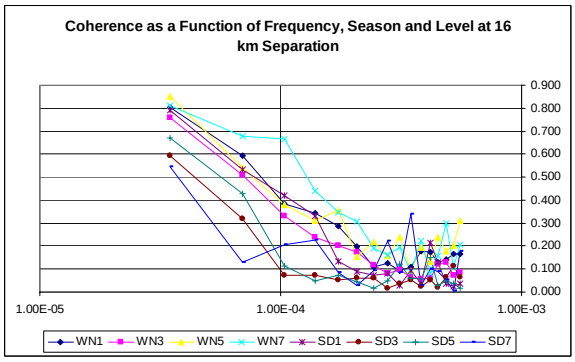

Figure 19. Coherence spectra for summer and winter at levels 1, 3, 5 and 7 for profiler pairs spaced 16 +/2 km.

At each level and frequency for each season, the coherence is generally lower when the spacing between profilers is larger. Figure 20 shows the coherence as a function of frequency and spacing for winter nights at level 3. This example is typical, and this behavior was expected.

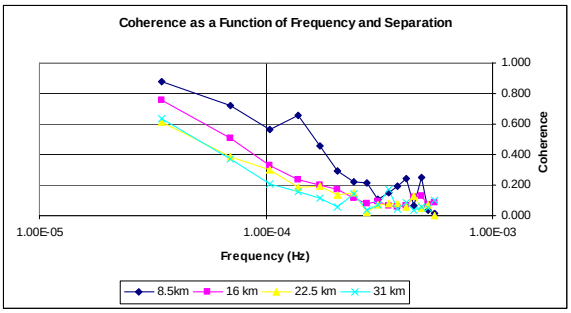

Figure 20. Coherence spectra for four separation distances for winter nights at level 3.

6.4 *Discussion*

At the longer time scales where the coherence is not too small to be significant, it does depend on separation as expected. This is consistent with results from higher in the atmosphere such as those of Merceret (2000) and Spiekerman *et al.* (2000) in that short distances are associated with short time scales.

Although those papers dealt with vertical spatial scales and temporal separations whereas this work examines temporal scales and horizontal separations, if one applies the same scaling relation found there, a two hour period would correspond to a coherence length of 16.5 km. The corresponding value from our data using Figure 20 is 8.5 km. This agreement within a factor of two may be coincidental, but it is suggestive that the previous work in the mid-troposphere and this work in the boundary layer are in quantitative agreement.

At higher frequencies (shorter time scales), the coherence falls below levels of practical significance. To the extent that these scales contribute to the wind variance at each profiler, that variance will be uncorrelated.

7. SUMMARY AND CONCLUSIONS

7.1 *Relation between temporal scale of motion and spatial coherence*

The most significant finding of this paper is that the spacing between the wind profilers in the KSC/CCAFS network is larger than the spatial scales of motion responsible for the wind variance at periods less than about two hours. All three methodologies are consistent with this conclusion. The spatial structure functions behave asymptotically with distance, the cross correlations are independent of separation distance at all lags up to two hours, and the coherence becomes small at frequencies larger than about 10^{-4} Hz. A two hour period corresponds to a frequency of 1.39×10^{-4} Hz.

7.2 *Seasonal and temporal dependence*

The contamination of the structure functions by the peculiar behavior of RWP 3 (see section 4.4) makes using these results difficult for examining seasonal and temporal effects, but no obvious differences appear in either the temporal or spatial structure functions except near the surface (level 1). Level 1 shows larger temporal structure functions during the day than at night, but no meaningful seasonal dependence. Excluding pairs involving RWP3, the winter spatial structure functions are also larger during the day than at night, but in the summer season there does not appear to be a significant diurnal effect even at level1.

The correlations showed a clear seasonal variation but no significant diurnal variation as noted in sections 5.2 and 5.3.

Due to the lack of spectral data from winter days and summer nights, diurnal comparisons of spectral data were not performed. There did not appear to be any seasonal dependence.

7.3 *Altitude dependence*

As might be expected from the trend for mean wind speeds to increase with altitude in the boundary layer, the spatial and temporal structure functions increase with altitude, except for level 1 which is directly subject to surface effects.

The autocorrelations do not appear to vary significantly with height, but the cross correlations do show some height dependence. The winds are more highly cross correlated aloft than near the surface, most likely because local effects are diffused as the distance from the surface where they occur increases.

Except for suggestions of a noise floor in the power spectra at higher altitudes as discussed in section 6.2, there was no altitude dependence observed in the spectral analysis.

7.4 *Conclusions*

A major implication of section 7.1 is that measurements made by balloons or wind profilers at distances greater than 8.5 km from the launch site will be uncorrelated with the winds at the launch site on time scales of two hours or less. Features having longer time scales will be correlated to a degree increasing with their time scale.

Another finding of potential operational significance is that the data generally indicate the lowest level considered here to be more strongly influenced by direct, local surface conditions and phenomena than all of the levels above it. This suggests that for purposes of general characterization of the atmosphere for design purposes and instrumentation, the region below 600 m should be considered separately from the region between 600 and 3000 meters.

The analysis of the data presented here is in its early stages as this preprint is being prepared. It is anticipated that these preliminary findings will be refined, corrected when necessary, and extended prior to the presentation of the poster at the conference.

8. ACKNOWLEDGMENTS

The authors thank Stanley Adelfang of Morgan Research Group at Marshall Spaceflight Center for reformatting the data to facilitate the time series analysis. We also thank Winnie Lambert of ENSCO, Inc. at the Applied Meteorology Unit for providing Figure 1.

Mention of a proprietary product or service does not constitute an endorsement thereof by the authors, the National Aeronautics and Space Administration, or the American Meteorological Society.

9. REFERENCES

Lambert, W.C., F.J. Merceret, G.E. Taylor and Jennifer G. Ward, 2003: Performance of Five 915-MHz Wind Profilers and an Associated Automated Quality Control Algorithm in an Operational Environment, *J. Atm. & Ocean. Tech.,* **20(11)**, 1488-1495.

Merceret, Francis J.,1995: The Effect of Sensor Spacing on Wind Measurements at the Shuttle Landing Facility, NASA Technical Paper 3529.

Merceret, Francis J., 1997: Rapid Temporal Changes of Midtropospheric Winds*. J. Appl. Meteor*., **36(11)**, pp. 1567 - 1574.

Merceret, Francis J., 2000: The Coherence Time of Mid-Tropospheric Wind Features as a Function of Vertical Scale from 300m to 2 Km, *J. Appl. Meteor.,* **39**, 2409-2420.

Spiekerman, C.E., B.H. Sako and A.M. Kabe (2000): Identifying Slowly Varying and Turbulent Wind features for Flight Loads Analysis, *J. Spacecraft and Rockets*, **37**, 426-433.

Stull, R.B., 1988: *An Introduction to Boundary Layer Meteorology*, Kluwer Academic Publishers, 670 pp.